Thirty-Third Hanford Symposium
on Health and the Environment

In-Situ Remediation: Scientific Basis for Current and Future Technologies

November 7-11, 1994
Pasco, Washington, U.S.A.

Part 2

Edited by
Glendon W. Gee and N. Richard Wing

BATTELLE PRESS
Columbus * Richland

MODELING EQUILIBRIUM AND KINETIC MAJOR ION CHEMISTRY WITH CO_2 PRODUCTION/TRANSPORT COUPLED TO UNSATURATED WATER FLOW

D. L. Suarez and J. Šimůnek

U.S. Salinity Laboratory, U.S. Department of Agriculture, Agricultural Research Service, Riverside, California

Key words: *Carbon dioxide, multicomponent transport, ionic exchange*

ABSTRACT

Modeling the aqueous-phase composition in the unsaturated zone requires prediction of the gas-phase composition as well as water flow and chemical reactions. We discuss and demonstrate the use of two finite-element codes developed for variably saturated media at near earth-surface temperature. The SOILCO$_2$ code was designed for predicting the CO_2 concentration in the unsaturated zone, while the UNSATCHEM-2D code was designed for predicting major ion composition in the unsaturated zone. The SOILCO$_2$ code couples CO_2 production and transport with a variably saturated water flow model. The UNSATCHEM-2D code couples a variably saturated water flow model to CO_2 production and transport, solute transport, and major-ion chemistry submodels. Since the solution chemistry in the unsaturated zone is significantly influenced by variations in water content, and in temperature and CO_2 concentrations in the soil gas, all these variables are calculated by the models. The CO_2 transport submodel includes both liquid and gas-phase transport.

The production submodel accounts for microbial and root respiration of CO_2, both of which are dependent on water content, temperature, salinity, and plant and soil characteristics. The chemistry submodel accounts for equilibrium reactions such as complexation, cation exchange, and precipitation-dissolution among the major chemical species. In addition, the user can select either equilibrium or multicomponent kinetic expressions for precipitation-dissolution of calcite and dissolution of dolomite. Dissolution-precipitation reactions are also included for gypsum, and for various carbonate and silicate phases.

Modified Debye-Hückel as well as Pitzer expressions were incorporated into the submodel to calculate single-ion activities for the range of dilute to hypersaline waters. Examples are presented to demonstrate the applicability of the codes for predicting CO_2 concentrations and transport, and for simulating soil chemical processes and changes in dissolved major ion composition with time and depth.

INTRODUCTION

Prediction of groundwater quality requires consideration of the chemical composition of recharge water. This, in turn, requires modeling of water flow and solute transport, as well as pertinent chemical processes in the unsaturated zone. This modeling is especially important for environmental concerns related to human activities, where steady-state assumptions are not likely to be valid. Realistic modeling of chemical processes in the unsaturated zone requires consideration of processes in the gas, liquid, and solid phases. Among the important factors influencing chemical dynamics in the unsaturated zone are water flow, heat transport, and dynamic changes in CO_2 concentrations. Water is not only the transport medium for inorganic dissolved chemicals but also significantly affects the production and concentration of CO_2. Soil temperature affects thermodynamic constants and reaction rates and, more importantly, the production of CO_2. The CO_2 concentration exerts a major control on the biological and chemical processes in the soil, and has a direct effect on the solution chemistry of the entire subsurface. Variations in soil CO_2 concentration produce changes in soil pH (for all but acid soils), and thus alter the solubility of many solid phases (e.g., carbonates and oxyhydroxides), and the transport of species whose absorption is pH-dependent.

Over the past two decades a large number of models have been developed to quantify the physical and chemical processes affecting major ion transport. Hydrological models for water flow, solute transport, and aqueous equilibrium chemistry were developed independently of one another, and only recently has there been a significant effort to couple these models. Solute transport models typically considered only one solute and greatly simplified the different chemical processes (Yeh and Huff, 1985; Huyakorn et al., 1991). For example, the complex processes of adsorption and cation exchange were usually accounted for by linear or Freundlich isotherms, where all reactions between solid and liquid phases were lumped into a distribution coefficient, K_D, and possibly into the nonlinear exponent, so that the adsorption processes were modeled independently of the behavior of other solution species. Other processes, such as precipitation, biodegradation, volatilization or radioactive decay, were simulated by simple first- or zero-order rate constants. Several models were developed that simulate several solutes involved in sequential first-order decay reactions (Gureghian, 1981; Wagenet and Hutson, 1987; Šimůnek and van Genuchten, 1994).

Researchers have also addressed the problem of coupling hydrological models for water flow and solute transport with chemical equilibrium models. Recent reviews of hydrogeochemical transport models that consider multiple reactive chemical components were presented by Yeh and Tripathi (1989) and Mangold and Tsang (1991). Until now, most of the models were developed for saturated water flow where changes in water velocity, temperature, and pH are relatively gradual and hence less important than in the unsaturated zone. Therefore, most models are based on one-dimensional, steady-state, saturated water flow with fixed water velocity, temperature, and pH (e.g. Valocchi et al., 1981; Jennings et al., 1982; Walsh et al., 1984; Cederberg et al., 1985; Kirkner et al., 1985; Bryant et al., 1986; Förster and Gerke, 1988). Only recently were several models published that can be applied to problems that include multicomponent reactive solute transport and variably saturated water flow (Liu and Narasimhan, 1989; Yeh and Tripathi, 1991). In addition, Robbins et al. (1980a,b) developed chemical precipitation-dissolution and cation exchange subroutines using equilibrium chemistry, and coupled them with a one-dimensional water movement, salt transport, and plant growth model. Robbins' equilibrium chemistry model was also the basis for the numerical code LEACHM of Wagenet and Hutson (1987).

The chemical reaction and multicomponent transport models described above use either the total inorganic carbon as a conservative property and/or fixed pH as an input variable. This approach can be used only for closed systems, which makes it applicable to the chemistry of only some groundwater systems (Suarez, in press); nonetheless, it has also been applied to open systems such as soil environments. The alternative assumption of an open system with fixed CO_2 is preferable to an assumption of fixed pH, but it suffers from not accounting for the dynamics of the gas phase. In the unsaturated zone, the CO_2 concentration varies in space and time, resulting in increases in dissolved inorganic carbon and decreases in soil pH when CO_2 increases. Use of the open system, variable CO_2 concentration (that allows for transfer of carbon into or out of the system), and the use of alkalinity as an input variable is preferable, because alkalinity is conserved during changes in soil CO_2 (and is transferred to the solid phase during precipitation).

Since the assumption of time-invariant CO_2 is often not realistic, there is a need to couple multicomponent models not only to variably saturated water flow and solute transport models, but also to CO_2

transport-production models. Modeling of the spatial distribution and fluxes of CO_2 has been limited and was undertaken mostly through statistical correlation with specific parameters such as air or soil temperature, latitude, and soil water content. Recently, process-oriented models were developed that are suitable to predict the transport and distribution of CO_2 (Ouyang and Boersma, 1992; Šimůnek and Suarez, 1993a). Šimůnek and Suarez (1993a) developed the SOILCO2 model, which considers variably saturated water flow, heat and CO_2 transport, and biological CO_2 production. In a companion paper, Suarez and Šimůnek (1993) evaluated the sensitivity of the model to the input parameters and recommended values to be used for the parameters.

Another consideration is that most earlier models treat only equilibrium reactions, while published data for natural systems indicate that reaction rates often control solution composition. For example, studies of major ion compositions in the unsaturated and shallow groundwater zones beneath calcareous soils in arid zones show that calcite equilibrium is not a reasonable assumption for predicting water composition (Suarez, 1977; Suarez and Rhoades, 1982) and that a kinetic expression yields values closer to field measurements (Suarez, 1985).

The UNSATCHEM-2D code developed by Šimůnek and Suarez (1994) couples the two-dimensional, variably saturated water flow and solute transport model SWMS-2D (Šimůnek et al., 1992) with a much expanded version of the speciation model CARBCHEM (Suarez, 1977) and the two-dimensional version of the CO_2 transport and production model SOILCO2 (Šimůnek and Suarez, 1993a). The chemical speciation model was modified and expanded into a predictive model. The model differs fundamentally from a pure equilibrium model in that only processes that have been demonstrated to be represented by the equilibrium condition are treated as equilibrium processes. The model is limited only to the species, solids, and processes or reactions that have been evaluated for field conditions. The model now includes options for forcing equilibrium with various solid phases (e.g., gypsum, calcite, dolomite, nesquehonite, and hydromagnesite), allowing the solution to precipitate various solid phases if saturation is reached, or utilizing rate equations for calcite precipitation/dissolution and dolomite dissolution. We consider that gypsum, nesquehonite or hydromagnesite, if present, are likely to equilibrate with the solution phase. Calcite, and particularly dolomite, cannot be assumed to be in equilibrium with the solution phase. The UNSATCHEM-2D model (Šimůnek

and Suarez, 1993b) is only applicable to nonacid environments with pH > 6. The 1-D version under development (Suarez and Šimůnek, in preparation) is applicable to the full range of pH values and includes silicate weathering reactions, aluminium species, gibbsite, as well as functions that describe changes in hydraulic properties due to chemical conditions.

In the following sections we present the basic equations and a brief discussion of the variably saturated water flow, CO_2 production and transport, and multicomponent solute transport of the UNSATCHEM-2D and SOILCO$_2$ codes. Detailed descriptions of the codes and numerous test cases are given in the referenced papers and user manuals. Emphasis here is given to the CO_2 transport and production and to the chemical submodel. We also present examples that demonstrate the applicability of SOILCO$_2$ for predicting CO_2 transport and production, and of UNSATCHEM-2D for simulating the precipitation of calcite and movement of an exchange front in the soil as a function of depth and time.

MODEL DEVELOPMENT

Variably Saturated Water Flow

Two-dimensional isothermal Darcian flow of water in a variably saturated rigid porous medium is described by a modified form of the Richards equation, with the assumptions that the air phase plays a negligible role in the liquid flow process and that the soil matrix and fluid are incompressible:

$$\frac{\partial \theta}{\partial t} = \frac{\partial}{\partial x_i}\left[K\left(K_{ij}^{A}\frac{\partial h}{\partial x_j} + K_{iz}^{A}\right)\right] - S, \qquad (1)$$

where θ is the volumetric water content (L^3L^{-3}), h is the pressure head (L), S is a sink term representing root water uptake (T^{-1}), x_i (i=1,2) are the spatial coordinates (L), t is time (T), K_{ij}^{A} denotes components of a dimensionless anisotropy tensor K^A, K is the unsaturated hydraulic conductivity function (LT^{-1}), and z represents the vertical coordinate (L).

The sink term, S, in equation (1) represents the volume of water removed per unit time from a unit volume of soil due to plant water uptake. The expression for S proposed by Feddes et al. (1978) and subsequently modified to include salinity stress (van Genuchten, 1987) is

$$S(h, h_\phi, x, z) = a_h(h)\, a_\phi(h_\phi)\, S_p(x, z), \tag{2}$$

where the dimensionless water and salinity stress response functions $a_h(h)$ and $a_\phi(h_\phi)$ depend on the soil water pressure head, h ($0 \le a_h \le 1$), and osmotic head, h_ϕ ($0 \le a \le 1$) [see van Genuchten (1987) for a detailed description], respectively, and $S_p(x,z)$ is the potential water uptake rate at coordinates x, z (T^{-1}). The actual water uptake, S(x,z), is equal to the potential uptake rate, $S_p(x,z)$, during periods of no water and salinity stress (i.e., when $a_h(h) = a_\phi(h_\phi) = 1$). Values for the osmotic head are obtained using osmotic coefficients and a modified form of the van't Hoff equation (Suarez and Šimůnek, in preparation).

The potential water uptake rate in the root zone, $S_p(x,z)$, depends on the root density at the particular depth. $S_p(x,z)$ can be expressed as the product of the potential transpiration rate, T_p (LT^{-1}), and the normalized water uptake distribution function, $\beta(x,z)$ (L^{-2}), which describes the spatial variation of the potential water uptake rate, S_p, over the root zone:

$$S_p(x, z) = \beta(x, z)\, T_p\, L_t, \tag{3}$$

where L_t is the length of the soil surface associated with transpiration.

There are many ways to express the function $\beta(x,z)$; e.g., van Genuchten (1987) suggested the following one-dimensional depth-dependent root distribution function $\beta(z)$:

$$\begin{aligned} \beta(z) &= \frac{5}{3L_r} && z \le 0.2L_r \\ \beta(z) &= \frac{25}{12L_r}\left(1 - \frac{z}{L_r}\right) && 0.2L_r < z \le L_r \\ \beta(z) &= 0 && z > L_r, \end{aligned} \tag{4}$$

where L_r is the root depth (L). Note that integrating both sides of equation (3) with respect to space, using equation (4) for $\beta(x,z)$ ($=\beta(z)/L_t$), shows that the potential transpiration for the entire soil profile is given by the integral of $S_p(x,z)$ over space (the function $\beta(x,z)$ integrates to unity over the rooting volume). The actual transpiration rate, T_a (LT^{-1}), is similarly obtained by integrating the root water uptake rate over the root zone as follows:

$$T_a = \frac{1}{L_t}\int_{\Omega_R} S(h,x,z)\,d\Omega = T_p \int_{\Omega_R} \alpha_h(h)\,\alpha_\phi(h_\phi)\,\beta(x,z)\,d\Omega\,, \tag{5}$$

where Ω_R is the region occupied by the root zone.

The root depth, L_r [L], can be either constant or variable during the simulation. For annual vegetation, a growth model is required to simulate the change in rooting depth with time. In this model we consider the root depth to be the product of the maximum rooting depth, L_m [L], and the dimensionless root growth coefficient, $f_r(t)$:

$$L_r(t) = L_m f_r(t)\,. \tag{6}$$

To calculate the root growth coefficient, $f_r(t)$, we combined the Verhulst-Pearl logistic growth function with the growth degree day (GDD) (Gilmore and Rogers, 1958). The logistic growth function describes biological growth at constant temperature, whereas the GDD model is typically utilized for determining the time interval between planting and maturity of the plant. Thus, to model the root growth for changing temperature we scale the time in the logistic growth function by the GDD function.

For the GDD function we used a modified version of the relation developed by Logan and Boyland (1983), who assumed that this function is fully defined by the temperature, T (K) (which can be expressed by a sine function to approximate the behavior of temperature during the day), and by three temperature limits, T_1, T_2, and T_3. When the actual temperature is below the base value T_1, plants register no effective growth. Between temperatures T_1 and T_2, plant growth increases from zero to the maximum value. Plant growth is at a maximum level at temperature T_2 and remains unchanged within the interval up to a maximum temperature, T_3. Above T_3, increased temperature has a negative effect on growth. Based on this reasoning we developed the following dimensionless growth function:

$$GDD(t) = \begin{cases} 0 & t \le t_p\,;\ t \ge t_h \\ \dfrac{1}{T_{Bas}}\left[\int \delta(T-T_1)\,dt - \int \delta(T-T_2)\,dt - \int \delta(T-T_3)\,dt\right] & t \in (t_p, t_a)\,, \\ 1 & t \in (t_a, t_h) \end{cases} \tag{7}$$

where T_{max} are the heat units (KT) necessary for the plant to mature and the roots to reach the maximum rooting depth; t_p, t_m, and t_h represent time of planting, time at which the maximum rooting depth is reached, and time of harvesting, respectively. The parameter δ introduces into the GDD the reduction of the instantaneous heat unit contributions due to water and osmotic stress. The individual integrals in equation are evaluated only when particular arguments are positive. Parameter δ is defined as the ratio of the actual to potential transpiration rates:

$$\delta = \frac{T_a}{T_p}. \tag{8}$$

Biomass or root development during plant growth can also be expressed by the classical Verhulst-Pearl logistic growth function:

$$f_r(t) = \frac{L_0}{L_0 + (L_m - L_0)\, e^{-rt}}, \tag{9}$$

where L_0 is the initial value of the rooting depth at the beginning of the growth period (L), and r is the growth rate constant (T^{-1}).

Growth functions, equations (7) and (9), can both be used directly to model the root growth. However as discussed above, to avoid limitations in both concepts, we combine equations (7) and (9) by substituting the growth function calculated from the heat unit concept (7) for the time parameter in the logistic growth function [equation (9)] as follows:

$$t = t_m\, GDD(t), \tag{10}$$

where t_m is the time when GDD reaches the required value for the specific plant species (T_{max}). This value is not known a priori, however; only the product rt_m must be known, and that can be selected, for example, so that $f_r(t)$ equals 0.99 for GDD(t) = 1.

Multicomponent Solute Transport

The partial differential equation governing two-dimensional advective-dispersive chemical transport under transient water flow condi-

tions in partially saturated porous media is taken as (Šimůnek and Suarez, 1994)

$$\frac{\partial(\theta c_k)}{\partial t} + \rho\frac{\partial \bar{c}_k}{\partial t} + \rho\frac{\partial \hat{c}_k}{\partial t} = \frac{\partial}{\partial x_i}\left(\theta D_{ij}\frac{\partial c_k}{\partial x_j} - q_i c_k\right) \qquad k = 1, 2, \ldots, N_c, \tag{11}$$

where c_k is the total dissolved concentration of aqueous component k (ML^{-3}), $\bar{c}_k$ is the total sorbed concentration of component k (MM^{-1}), $\hat{c}_k$ is the total solid-phase concentration of component k (MM^{-1}), ρ is the bulk density of the medium (ML^{-3}), D_{ij} is the "effective" dispersion tensor (L^2T^{-1}), q_i is the volumetric soil water flux (LT^{-1}), and N_c is the number of aqueous components. Solute uptake by plant roots is not considered in equation (11), as plants take up a negligible fraction of the salts present in the soil water. Equation (11) also assumes that the aqueous component does not undergo any decay or production reactions. The second and third terms on the left side of equation (11) are zero for components that do not undergo ion exchange (which is the only sorption-type interaction for these species) or precipitation/dissolution.

Carbon Dioxide Transport

Modeling CO_2 transport in the unsaturated zone requires consideration of both liquid- and gas-phase transport. Furthermore, we consider that the CO_2 is transported via two mechanisms (Patwardhan et al., 1988), convective transport in the aqueous phase and diffusive transport in both gas and aqueous phases, and that the concentration is affected by both CO_2 production and removal. Thus, the two-dimensional CO_2 transport is described by the following mass balance equation:

$$\frac{\partial(c_a\theta_a + c_w\theta)}{\partial t} = \frac{\partial}{\partial x_i}\left(\theta_a D_{ij}^a\frac{\partial c_a}{\partial x_j}\right) + \frac{\partial}{\partial x_i}\left(\theta D_{ij}^w\frac{\partial c_w}{\partial x_j}\right) - \frac{\partial}{\partial x_i}(q_i c_w) - Sc_w + P, \tag{12}$$

where c_w and c_a are the volumetric concentrations of CO_2 in the solution phase and gas phase (L^3L^{-3}), respectively; D_{ij}^a is the effective soil matrix diffusion coefficient tensor of CO_2 in the gas phase (L^2T^{-1}); D_{ij}^w is the effective soil matrix dispersion coefficient tensor of CO_2 in the solution phase (L^2T^{-1}); q_i is the volumetric soil water flux (LT^{-1}); θ_a is the volumetric air content (L^3L^{-3}); and P is the CO_2 production rate ($L^3L^{-3}T^{-1}$). The term Sc_w represents the dissolved CO_2 removed from the soil by root water uptake. This term is necessary because, when plants take up water, the dissolved CO_2 is also taken up by the plant roots. The

volumetric concentrations of CO_2 in the solution and gas phases are related by the equation

$$c_w = K_c c_a, \tag{13}$$

where K_c is the distribution constant, which is strongly dependent on temperature. Šimůnek and Suarez (1993a) defined the total aqueous-phase concentration of CO_2, c_w, as the sum of CO_2(aq) and H_2CO_3, and related it to the CO_2 concentration in the gas phase, c_a, with a modified Henry's Law. However, aqueous carbon also exists in the form of dissociated carbonic acid, HCO_3^-, CO_3^{2-}, as well as other species, such as $CaCO_3^o$, and these species should be included in the expression for c_w. Partitioning of total carbon or alkalinity into these species requires a fairly detailed chemical speciation program and thus cannot be considered in a strictly gas-water transport model (such as SOILCO2) but requires a model that includes chemical reactions and speciation (such as UNSATCHEM-2D). It is therefore suggested that UNSATCHEM-2D be used rather than SOILCO2 whenever solution species composition is available.

Carbon Dioxide Production

We treat CO_2 production as the sum of microbial and plant root respiration. It is assumed that it is possible to superpose the effects of environmental variables that alter the biological production from the reference value under optimal conditions (Šimůnek and Suarez, 1993a). The production of CO_2 is then taken as the sum of the production rate by the soil microorganisms, γ_s ($L^3L^{-3}T^{-1}$), and the production rate by plant roots, γ_p ($L^3L^{-3}T^{-1}$).

$$P = \gamma_s + \gamma_p = L_{ps}\,\gamma_{s0} \prod_i f_{si} + L_{pp}\,\gamma_{p0} \prod_i f_{pi} \quad \text{and} \tag{14}$$

$$\prod_i f_{ji} = f_j(x,z)\, f_j(h)\, f_j(T)\, f_j(c_a)\, f_j(h_\phi)\, f_j(t) \qquad j = p, s, \tag{15}$$

where the subscript s refers to soil microorganisms, and the subscript p refers to plant roots, πf_μ is the product of reduction coefficients that depends on depth (L^{-2}), pressure head (or the soil water content) (-),

temperature (-), CO_2 concentration (-), osmotic head (-) and time (-), and L_N is the width (L) of the soil surface associated with the CO_2 production processes. The parameters γ_{s0} and γ_{p0} represent the CO_2 production by the soil microorganisms or plant roots, respectively, for the entire soil profile at 20°C under optimal water, solute, and CO_2 concentration conditions ($L^3L^{-3}T^{-1}$). Detailed discussion of the optimal production value, as well as coefficients for the reduction functions are given in Suarez and Šimůnek (1993).

The CO_2 production by microorganisms decreases sharply with depth as a result of a decrease in root mass and readily decomposable organic matter. There are many available one-dimensional expressions which can be utilized to relate the dependence of the CO_2 production term $f_s(x,z)$ on soil depth, including the exponential distribution with depth:

$$f_s(x,z) = \frac{a e^{-az}}{L_{ps}}, \tag{16}$$

where a is an empirical constant (L^{-1}). The exponential function is multiplied by the constant a in order to ensure that the integral of the function $f_s(x,z)$ from the soil surface to infinite depth is equal to unity. However, because the depth of the soil profile or the root depth is finite, the distribution function $f_s(x,z)$ must always be normalized. We assume that the dependence of the CO_2 production by plant roots corresponds to the root growth function $L_r(t)$ and the distribution function $\beta(x,z)$ used for the water uptake by plant roots.

In view of the experimental data of Williams et al. (1972) and Rixon (1968), the CO_2 reduction coefficient $f_s(h)$ as a function of the soil water pressure head for soil microorganisms is expressed as

$$\begin{aligned} f_s(h) &= 1 && h \in (h_2, +\infty) \\ f_s(h) &= \frac{\log|h| - \log|h_3|}{\log|h_2| - \log|h_3|} && h \in (h_3, h_2) \\ f_s(h) &= 0 && h \in (-\infty, h_3), \end{aligned} \tag{17}$$

where h_2 is the pressure head when CO_2 production is optimal (L) and h_3 is the pressure head when production ceases (L). The dependence of

the reduction terms $f_p(h)$ and $f_p(h_o)$ on soil water pressure head and osmotic head, respectively, are represented by expressions similar to the reduction functions described for water uptake (namely, $a_h(h)$ and a_o).

The influence of temperature on chemical processes is described by the Arrhenius equation (Stumm and Morgan, 1981):

$$\ln q = -E/RT + a, \tag{18}$$

where T is absolute temperature (K), E is the activation energy of the reaction ($ML^2T^{-2}M^{-1}$), and q is the reaction rate constant. In our model, q represents the CO_2 production rate. This equation, together with the Van't Hoff equation, has been used by many authors to represent the influence of temperature on soil and root CO_2 production. Assuming that $f_j(T) = 1$ for $T_{20} = 293.15$ K, then the temperature reduction coefficient can be expressed as

$$f_j(T) = \exp\left[\frac{E_j(T - T_{20})}{RTT_{20}}\right] \qquad j = s, p. \tag{19}$$

The use of the term "reduction" coefficient with $f_j(T)$ may seem inappropriate, since this coefficient is higher than 1 for temperatures greater than 20°C. We use the term to characterize the change in production with temperature, with values greater than 1 above 20°C and less than 1 below 20°C.

The dependence of CO_2 production on its own concentration (actually, O_2 deficiency) can be obtained from an expression for the rate at which oxygen utilized by respiration is consumed as a function of oxygen concentration in the soil gas phase. The combined volumetric content of O_2 and CO_2 in the soil gas phase is assumed to be constant at 21%. The rate of oxygen uptake for respiration can be expressed with the Michaelis-Menton equation (Glinski and Stepniewski, 1985):

$$q = \frac{q_{max}}{1 + (K_M / c_{O_2})}, \tag{20}$$

where K_M is the Michaelis' constant (L^3L^{-3}), i.e., the oxygen concentration, c_{O_2}, at which the oxygen uptake is equal to 1/2 q_{max}, and where q is oxygen uptake rate, and q_{max} is the maximum oxygen uptake rate ($L^3L^{-3}T^{-1}$). Assuming that the respiratory quotient (i.e., the amount of

CO_2 produced per amount of O_2 consumed) is equal to unity, the Michaelis' constant for the CO_2 concentration, K_M^*, is then equal to $0.21\text{-}K_M$, and $c_a = 0.21 - c_{O_2}$. The reduction coefficient is then given by

$$f_j(c_a) = \frac{c_{O_2}}{c_{O_2} + K_{Mj}} = \frac{0.21 - c_a}{0.42 - c_a - K_{Mj}^*} \qquad j = s, p. \tag{21}$$

The disadvantage of this expression is that if $c_a = 0$, the value for $f_j(c_a)$ is not equal to one. Therefore, the values of the optimal production γ_{p0} and γ_{s0} must be adjusted accordingly.

The coefficient $f_j(t)$ introduces a time dependence into the production term. This coefficient should describe the diurnal and seasonal dynamics of soil and plant respiration. We assume that the diurnal dynamics for both soil and plant respiration are reflected by the temperature dependence coefficient $f_j(T)$ and that the seasonal dynamics of soil microorganism production of CO_2 is sufficiently described by other reduction coefficients. Therefore, we use this coefficient only for the description of the changes in CO_2 production caused by the different growth stage of plants. For example, we use the same approach for annual vegetation as we used for root growth [equations (7) through (9)]. The coefficient $f_j(t)$ can either be described in the same way as coefficient GDD(t) when the GDD concept is used [equation (7)], possibly with different constants, or in combination with the classical Verhulst-Pearl logistic function [equation (9)]. In this case, the maximum and initial values of the root depth should be replaced by the corresponding values of CO_2 production by plant roots.

The calculated actual CO_2 production rate, P_T, is obtained by integrating the CO_2 production throughout the whole soil profile as follows:

$$P_T = \int_\Omega P\,d\Omega = L_{ps}\,\gamma_{s0}\,f_s(t) \int_\Omega f_s(x,z)\,f_s(h)\,f_s(T)\,f_s(c_a)\,f_s(h_\phi)\,d\Omega + L_{pp}\,\gamma_{p0}\,f_p(t) \int_\Omega f_p(x,z)\,f_p(h)\,f_p(T)\,f_p(c_a)\,f_p(h_\phi)\,d\Omega. \tag{22}$$

Solution Chemistry

As mentioned in the introduction, UNSATCHEM-2D is only applicable to nonacid environments with a pH > 6 (Šimůnek and Suarez, 1993b, 1994), and UNSATCHEM-1D can be used for acid as well as alkaline

environments (Suarez and Šimůnek, in preparation). The chemical species that are considered in the codes are given in Table 1; species that are only considered in the 1-D code are highlighted. The chemical system for predicting major ion solute chemistry of the unsaturated zone includes either 37 or 55 chemical species (depending on the pH range) as listed in Table 1: 10 aqueous chemical components (calcium, magnesium, sodium, potassium, sulfate, chloride, nitrate, aluminum, silica, and organic matter), 25 complex aqueous species, seven possible solid species (calcite, gypsum, nesquehonite, hydromagnesite, dolomite, sepiolite, and gibbsite), six sorbed species, and seven species constituting the CO_2-H_2O system.

Mass balance equations for the major components in the first group of Table 1 are defined as the sum of the corresponding constituent species. In addition to 10 mass balance equations for major components, two mass balance equations for the total analytical concentration of carbonate and bicarbonate are defined:

$$CO_{3_T} = [CO_3^{2-}] + [CaCO_3^0] + [MgCO_3^0] + [NaCO_3^-]$$
$$HCO_{3_T} = [HCO_3^-] + [CaHCO_3^+] + [MgHCO_3^+] + [NaHCO_3^0], \quad (23)$$

Table 1. Species considered in the chemical submodel.

1	Aqueous components	10	Ca^{2+}, Mg^{2+}, Na^+, K^+, SO_4^{2-}, Cl^-, NO_3^-, $H_4SiO_4^0$, Al^{3+}, Org^-
2	Complexed species	25	$CaCO_3^0$, $CaHCO_3^+$, $CaSO_4^0$, $MgCO_3^0$, $MgHCO_3^+$, $MgSO_4^0$, $NaCO_3^-$, $NaHCO_3^0$, $NaSO_4^-$, KSO_4^-, $H_2SiO_4^{2-}$, $H_3SiO_4^-$,
			$AlSO_4^+$, $Al(SO_4)_2^-$, $AlHSO_4^{2+}$, $AlOH^{2+}$, $Al(OH)_2^+$ $Al(OH)_3^0$, $Al(OH)_4^-$, $AlOrg^0$, $AlHOrg^+$, $HOrg^{2-}$, H_2Org^-, H_3Org^0, HSO_4^-
3	Precipitated species	7	$CaCO_3$, $CaSO_4 \cdot 2H_2O$, $MgCO_3 \cdot 3H_2O$, $CaMg(CO_3)_2$, $Mg_2Si_3O_7{}_5(OH) \cdot 3H_2O$, $Mg_5(CO_3)_4(OH)_2 \cdot 4H_2O$, $Al(OH)_3$
4	Sorbed species	6	$\overline{Ca}$, $\overline{Mg}$, $\overline{Na}$, $\overline{K}$, $\overline{Al}$, $\overline{H}$
5	Additional species	7	P_{CO_2}, $H_2CO_3^*$, CO_3^{2-}, HCO_3^-, H^+, OH^-, H_2O

where variables with subscript T represent the total solution concentration of that particular variable, and brackets refer to molalities (mol kg^{-1}). The expressions given above are used to calculate carbonate alkalinity, Alk (mol$_c$ kg^{-1}), as

$$Alk = 2CO_{3_T} + HCO_{3_T} + [OH^-] - [H^+]. \tag{24}$$

In addition to the mass balance equations, the charge balance equation for the solution is

$$\begin{aligned} &2[Ca^{2+}] + 2[Mg^{2+}] + [Na^+] + [K^+] + [CaHCO_3^+] + [MgHCO_3^+] + [H^+] + 3[Al^{3+}] \\ &+ 2[AlOH^{2+}] + 2[AlHSO_4^{2+}] + [AlOH_2^+] + [AlHOrg^+] + [AlSO_4^+] - 2[CO_3^{2-}] - [HSO_4^-] \\ &- [HCO_3^-] - 2[SO_4^{2-}] - [Cl^-] - [NO_3^-] - [OH^-] - 2[H_2SiO_4^{2-}] - [H_3SiO_4^-] - 3[Org^{3-}] \\ &- [NaCO_3^-] - [NaSO_4^-] - [KSO_4^-] - [Al(SO_4)_2^-] - [Al(OH)_4^-] - 2[HOrg^{2-}] - [H_2Org^-] = 0. \end{aligned} \tag{25}$$

The activities of the species present in solution at equilibrium are related by the equilibrium mass-action expressions. These include the expressions for the dissociation of water, and the first and second dissociation constants for carbonic acid. The solubility of CO_2(g) in water is governed by a modified Henry's law,

$$K_{CO_2} = \frac{(H_2CO_3^*)}{P_{CO_2}(H_2O)}, \tag{26}$$

where the activity of $CO_{2(g)}$ is expressed as partial pressure P_{co_2}, K_{co_2} is a modificed Henry's Law constant, and parentheses denote ion activities. The term H_2CO_3* represents both aqueous CO_2 and H_2CO_3. The value for P_{co_2} is calculated at each node and time step by the production-transport submodel.

Each complexation reaction for species in the second group of Table 1 is represented by equilibrium mass-action expression. For example, for the calcium sulfate complex:

$$K_1 = \frac{(Ca^{2+})(SO_4^{2-})}{(CaSO_4^\circ)}. \tag{27}$$

Partioning between the exchanger phase and the solution is described by a generalized Gapon equation for cation exchange (White and Zelazny, 1986),

$$K_{ij} = \frac{\bar{c}_i^{y+}}{\bar{c}_j^{x+}} \frac{(c_j^{x+})^{1/x}}{(c_i^{y+})^{1/y}}, \tag{28}$$

where y and x are the valences of species i and j, respectively, and K_{ij} is the Gapon selectivity coefficient. This equation is modified from the original Gapon expression by the substitution of ion activities for the concentration terms. Adsorbed concentrations are expressed in moles of charge per mass of dry soil (mol$_c$kg^{-1}). It is assumed that the cation exchange capacity, (mol$_c$kg^{-1}), is constant and independent of pH. The assumption of constant exchange capacity is not valid for soils containing large amounts of variable charge, such as oxisols, but is necessary in the present models to maintain conservation of mass.

The following solid phases constrain the aqueous-phase solution to equilibrium whenever the solids are specified or approached from oversaturation: gypsum, nesquehonite, hydromagnesite, sepiolite, and gibbsite. Precipitation-dissolution of calcite is optionally treated with either equilibrium or kinetic expressions. In the latter case, the equation corresponding to calcite equilibrium is omitted from the equilibrium system and the rate of calcite precipitation-dissolution is calculated from a rate equation, as described later. Dissolution of dolomite, also discussed later, is always considered to be a kinetic process and is not included in the system of equilibrium equations (because ordered dolomite does not precipitate under earth surface conditions). Discussion of the selection and consideration of these solids is given in Suarez and Šimůnek (in preparation). The precipitation or dissolution of gypsum, calcite (if considered in the equilibrium system), nesquehonite, hydromagnesite, sepiolite, and gibbsite in the presence of CO_2 is described in terms of the corresponding solubility products K_{SP}:

$$K_{SP}^{C} = (Ca^{2+})(CO_3^{2-}) \qquad \text{calcite} \tag{29}$$

$$K_{SP}^{G} = (Ca^{2+})(SO_4^{2-})(H_2O)^2 \qquad \text{gypsum} \tag{30}$$

$$K_{SP}^{N} = (Mg^{2+})\,(CO_3^{2-})\,(H_2O)^3 \qquad \text{nesquehonite} \qquad (31)$$

$$K_{SP}^{H} = (Mg^{2+})^5\,(CO_3^{2-})^4\,(OH^-)^2\,(H_2O)^4 \qquad \text{hydromagnesite} \qquad (32)$$

$$K_{SP}^{S} = \frac{(Mg^{2+})^2\,(H_4SiO_4)^3\,(OH^-)^4}{(H_2O)^{4.5}} \qquad \text{sepiolite} \qquad (33)$$

$$K_{SP}^{B} = \frac{(Al^{3+})\,(H_2O)^3}{(H^+)^3} \qquad \text{gibbsite,} \qquad (34)$$

where indexes C, G, N, H, S, and B refer to calcite, gypsum, nesquehonite, hydromagnesite, sepiolite, and gibbsite, respectively.

The equilibrium concentrations of Ca^{2+} and SO_4^{2-} in a gypsum system are obtained by solving the quadratic algebraic equation corresponding to equation (30). The concentrations of Ca^{2+}, Mg^{2+}, and HCO_3^- in equilibrium with carbonate solids, as well as Al^{3+} for gibbsite, are determined by solving cubic algebraic equations, as described in Šimůnek and Suarez (1993b).

Kinetic Model of Calcite Precipitation-Dissolution

The reaction rate of calcite precipitation-dissolution, R^C, in the absence of inhibitors such as "foreign ions" and dissolved organic matter, can be calculated with the rate equation of Plummer et al. (1978),

$$R^C = k_1(H^+) + k_2(H_2CO_3^*) + k_3(H_2O) - k_4\frac{K_{a_2}}{K_{SP}^C}(Ca^{2+})(HCO_3^-), \qquad (35)$$

where

$$k_4 = k_1 + \frac{1}{(H_S^+)}\left[k_2(H_2CO_3^*) + k_3(H_2O)\right], \qquad (36)$$

and where K_{a_2} is the second dissociation constant of carbonic acid, and k_1, k_2, and k_3 are temperature-dependent, first-order rate constants representing the forward reactions (mmol $cm^{-2}s^{-1}$); and k_4 is a function dependent on temperature, surface hydrogen ion activity, and CO_2 concentration representing the backward reactions (mmol $cm^{-2}s^{-1}$). The dissolution-precipitation rate R^C is expressed in mmol of calcite per cm^2 of

surface area per second. The term (H_s^+) is the H^+ activity at the calcite surface and is assumed to be equal to the (H^+) of the solution at calcite saturation. Whenever pH > 8 and P_{co_2} < 1.0 kPa, at 25°C, the following precipitation rate expression is considered more accurate (Inskeep and Bloom, 1985):

$$R^C = -11.82[(Ca^{2+})(CO_3^{2-}) - K_{SP}^C]. \quad (37)$$

The precipitation or dissolution rate of calcite is reduced by the presence of various inhibitors. Šimůnek and Suarez (1993b) developed a function for the reduction of the precipitation-dissolution rates due to surface poisoning by dissolved organic carbon, based on the experimental data of Inskeep and Bloom (1986). These surface reaction precipitation-dissolution models simulate undersaturated and supersaturated conditions, such as those existing in field environments, but are questionable from a mechanistic point of view for precipitation. Pedogenic calcite forms as a microcrystalline cement, often with occlusions of clay and organic matter, which suggests a heterogeneous nucleation mechanism either by microbial activity or by surface reactions on clay.

Kinetic Model of Dolomite Dissolution

The reaction rates of dolomite dissolution, R^D (mmol cm^{-2}s^{-1}), are calculated with the rate equation of Busenberg and Plummer (1982):

$$R^D = k_1(H^+)^{0.5} + k_2(H_2CO_3^*)^{0.5} + k_3(H_2O)^{0.5} - k_4(HCO_3^-), \quad (38)$$

where the temperature-dependent, first-order rate constants k_1, k_2, k_3 (mmol cm^{-2}s^{-1}), representing the forward reactions, and k_4 (mmol cm^{-2}s^{-1}), representing the back reaction, are given by Busenberg and Plummer (1982). The dissolution rate R^D is again expressed in mmol of dolomite per cm^2 of surface area per second. As mentioned earlier, we do not consider the precipitation of dolomite. Formation of protodolomite, which has been observed in hypersaline environments, can be treated as a mixture of magnesium carbonate and calcium carbonate, both of which are considered in our chemical model.

Activity Coefficients

Calculation of single-ion activity coefficients is specified by using either an extended version of the Debye-Hückel equation (Truesdell and Jones, 1974) or Pitzer expressions (Pitzer, 1979). The extended version

of the Debye-Hückel equation (Truesdell and Jones, 1974), used in the dilute to moderately saline concentration range, is given by

$$\ln \gamma = -\frac{Az^2\sqrt{I}}{1 + Ba\sqrt{I}} + bI, \tag{39}$$

where A and B are constants that depend only on the dielectric constant, density, and temperature; z is the ionic charge; a and b are two adjustable parameters; and I is the ionic strength.

$$I = 0.5 \sum_{i=1}^{M} z_i^2 m_i, \tag{40}$$

where M is the number of species in the solution mixture, m_i is molality, and z_i is valence. The adjustable parameters a and b for individual species are given by Truesdell and Jones (1974). Activities of neutral species are calculated as

$$\ln \gamma = a' I, \tag{41}$$

where a′ is an empirical parameter. The values of this parameter for neutral species are listed in Šimůnek and Suarez (1993b).

At high ionic strength activity coefficients can no longer be considered universal functions of ionic strength but are also dependent on the concentration of the various ions present in solution (Felmy and Weare, 1986). The activity coefficients can then be calculated with a virial-type expansion of the form (Pitzer, 1979):

$$\ln \gamma_i = \ln \gamma_i^{DH} + \sum_j B_{ij}(I)\, m_j + \sum_j \sum_k C_{ijk} m_j m_k + \dots, \tag{42}$$

where γ_i^{DH} is a modified Debye-Hückel activity coefficient (which is a universal function of ionic strength), and B_{ij} and C_{ijk} are specific coefficients for each ion interaction. This model is considered accurate even for solutions with very high ionic strength (up to 20 molal) and can be used down to infinite dilution.

Solution Strategy

The Galerkin finite-element method with linear basis functions is used to obtain a solution of the water flow and solute and CO_2 transport equations subject to the imposed initial and boundary conditions. The

"mass-conservative" iterative method proposed by Celia et al. (1990) is used for evaluating the water content term in equation (1). This method has been shown to provide excellent results in terms of minimizing the mass balance error. A detailed description of the solution of Richards' equation was given in Šimůnek et al. (1992). The finite-element method is also used to solve the heat (see Šimůnek and Suarez, 1993b), CO_2, and multicomponent solute transport equations. A detailed description of the numerical solution for these transport equations is given in Šimůnek and Suarez (1993b).

Computation of the solution speciation is done in a way that is fairly similar to that in WATEQ (Truesdell and Jones, 1974), a speciation model that does not consider solid and adsorbed phases. The inputs to the chemical submodel of UNSATCHEM-2D are the analytical concentrations of the major ions, alkalinity, adsorbed and solid-phase concentrations, water content, temperature, bulk density, and CO_2 partial pressure (calculated in the gas subroutine).

The governing solute transport equation (11) contains time-derivative terms for the total dissolved, sorbed, and solid-phase concentrations. Because of the second and third terms, the solute transport equation is highly nonlinear, and its solution requires an iterative process. Coupling between the transport and chemical submodules was performed by the so-called "2-step" method as described by Walsh et al. (1984), Cederberg et al. (1985), and Bryant et al. (1986) (and also used by Yeh and Tripathi (1991)). First, the discretized solute transport equation is solved by setting the second and third terms equal to zero for the equilibrium case, or by calculating the third term from equations (35) and (38) for the kinetic case. The newly calculated dissolved concentrations are then compared with the initial concentrations for this iteration, and the chemical module is called for those nodes where changes in concentrations were higher than a prescribed concentration tolerance. When the rate equations for calcite or dolomite are used, the chemical module is called for all nodes at the first iteration. The chemical module provides us with updated values of aqueous, solid-phase, and adsorbed concentrations. The new aqueous concentrations are checked against those calculated before the chemical module was called and, if outside the specified tolerance, a new iteration is performed. This iteration process is continued until the difference between the new and old concentration is less than the prescribed tolerance for all nodes.

APPLICATIONS OF THE SOILCO2 AND UNSATCHEM-2D MODELS

In this section we present two simulations. The first case compares water content and CO_2 predictions using the SOILCO2 model, with a published data set where the temperature and rainfall data were given, along with soil water content and gas composition (Suarez and Šimůnek, 1993). The second case demonstrates an application of the UNSATCHEM-2D model to a chemical problem with calcite precipitation and movement of an exchange front into the soil.

Prediction of CO_2 Concentrations—Field Experiment

The predictive capabilities of SOILCO2 were examined by comparing simulations to the field data published by Buyanovsky and Wagner (1983) and Buyanovsky et al. (1986) for wheat grown in Missouri. Buyanovsky and Wagner (1983) presented data for water and CO_2 dynamics in soil under three different cropping systems for the year 1982. In a subsequent paper, Buyanovsky et al. (1986) investigated annual cycles of CO_2 evolution into the atmosphere from a soil cultivated to wheat and related the CO_2 flux to plant development, considering the effects of temperature and water content. Since they did not provide the hydraulic characteristics of the soil, we used the soil texture description and the measured air porosity at field capacity, along with the regression equations developed by Rawls et al. (1982), to obtain a water content-pressure head relation for this soil.

The following example is taken from Suarez and Šimůnek (1993). Figure 1 shows the water content at the 0.2-m depth as reported by Buyanovsky and Wagner (1983), and the model prediction of water content with time at the same depth. Overall, the model provides a good fit to the experimental data, especially in view of the need to use Thornthwaite's equation (de Marsily, 1986) for the calculation of potential evapotranspiration and the method used to calculate the hydraulic parameters.

Figure 2 shows the excellent agreement between the measured CO_2 concentrations at the 0.2-m depth and the corresponding values calculated with the SOILCO2 code. There are no statistically significant differences between the measured and predicted CO_2 concentrations at the 90% confidence level. The irregular pattern in the CO_2 concentrations shown in Figure 2 can be understood if we consider both the soil temperature and the water content data shown in Figure 1. The CO_2

concentration is low during cold periods when production is low, as well as within relatively dry periods when the gas transport is high. During wet periods of moderate to warm temperatures, the CO_2 concentrations are relatively high (because of reduced transport and substantial production). The model was further tested against three other similar data sets from Missouri, and the fit was excellent in all cases.

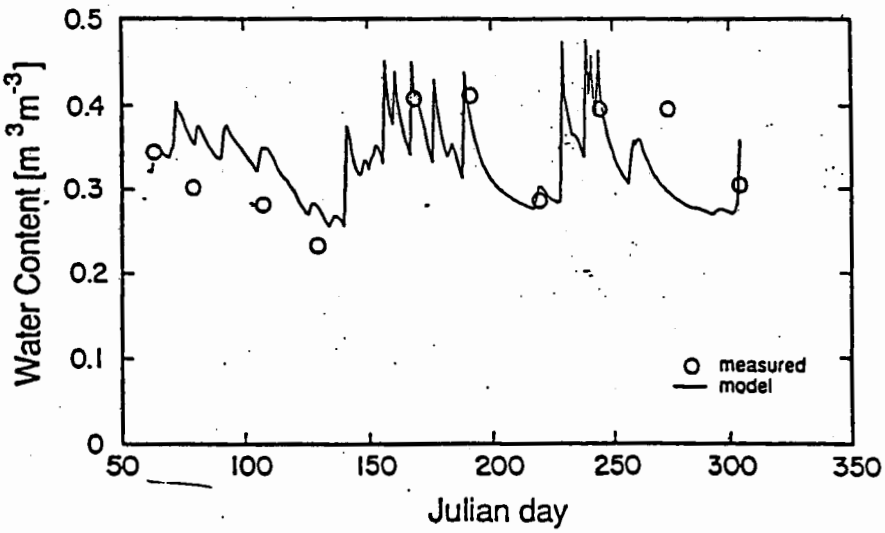

Figure 1. Measured (Buyanovsky and Wagner, 1983) and calculated water content at a depth of 0.2 m for Missouri wheat experiment (after Suarez and Šimůnek, 1993).

Figure 3 shows the comparison of the calculated daily and weekly CO_2 fluxes to the atmosphere with the flux measurements reported by Buyanovsky et al. (1986). We present the weekly values in addition to the daily values, because changes in the water content of the upper soil layer cause these rates to fluctuate significantly on a daily basis. The large fluctuations shown in Figure 3 indicate that accurate determination of CO_2 flux requires an excessive number of measurements if the surface water content is rapidly changing. This change in CO_2 flux is significant over time periods corresponding to rain events or water applications. As with the CO_2 concentration data, there is an excellent correspondence between measured and calculated fluxes.

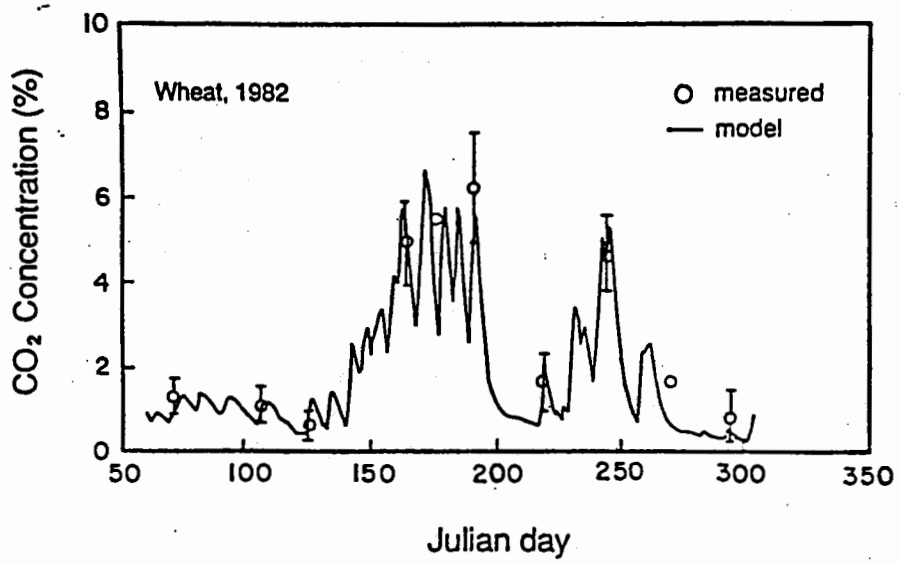

Figure 2. Measured (Buyanovsky and Wagner, 1983) and calculated CO_2 concentrations at a depth of 0.2 m for Missouri wheat experiment (after Suarez and Šimůnek, 1993).

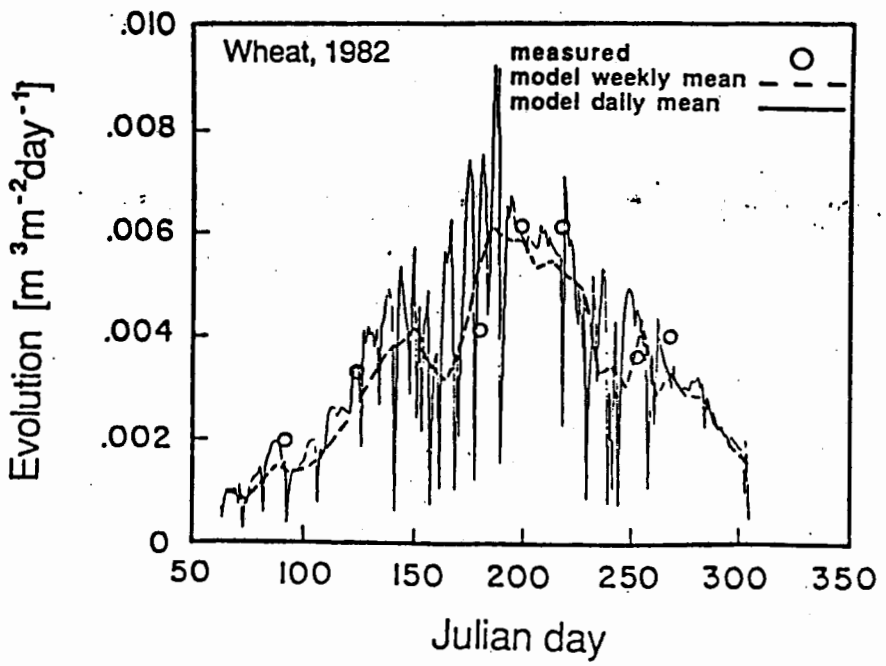

Figure 3. Measured (Buyanovsky and Wagner, 1983) and calculated daily and weekly CO_2 fluxes to the atmosphere for Missouri wheat experiment (after Suarez and Šimůnek, 1993).

Two-Dimensional Furrow Reclamation Irrigation Problem

A furrow irrigation system was used as a conceptual model of two-dimensional infiltration of water into a soil with high exchangeable sodium. The simulation demonstrates the cation exchange feature of UNSATCHEM-2D. The schematic representation of the flow domain for the furrow irrigation, together with the finite-element mesh, are presented in Figure 4. Because of symmetry, we need only simulate the domain between the axes of two neighboring furrows.

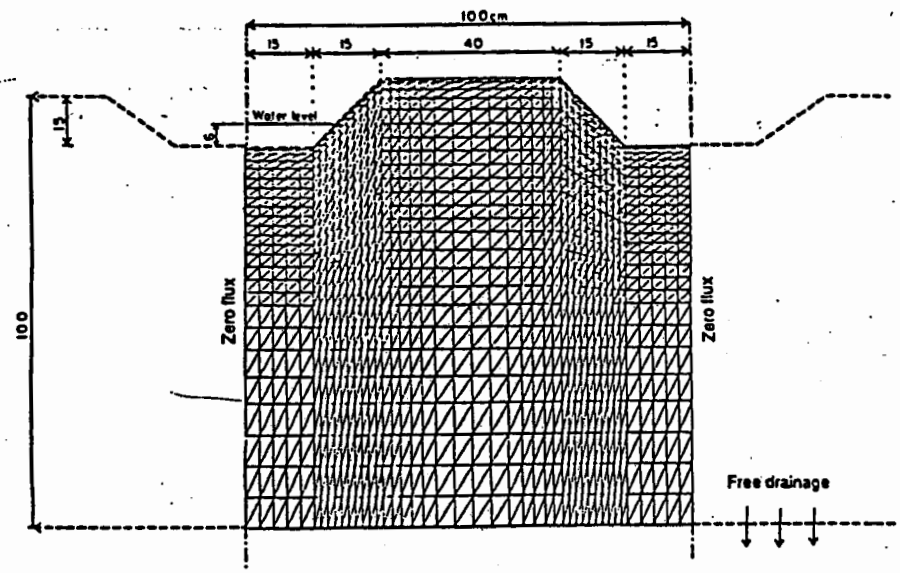

Figure 4. Schematic representation and finite-element mesh of the flow domain for furrow irrigation system for example 2.

It is assumed that every other furrow is flooded with water and that the water level in the irrigated furrow is kept at a constant level of 6 cm. A fixed head boundary condition is used for the portion of the boundary in contact with the flooding water in the furrow. Free drainage is used as the bottom boundary condition; a zero flux condition is used for the rest of the boundary. The initial pressure head is -200 cm, and the soil hydraulic properties for a hypothetical loam soil (Šimůnek and Suarez, 1993b) were used.

Root water uptake and evaporation were neglected (which also means that $\gamma_{p0} = 0$). The calculation was run at a constant temperature of 25°C, with an optimal CO_2 production value γ_{s0} of 0.007 $m^3m^{-2}d^{-1}$. Production decreased exponentially with depth, as described in Suarez and Šimůnek(1993). This production value was also modified by reduction coefficients calculated by the code according to environmental conditions (in this case, coefficients depending on pressure head and CO_2 concentration). The bulk density of the soil was taken as 1.4 g cm^{-3}, while a molecular diffusion coefficient in water for solute transport of 2 cm^2d^{-1} was chosen. Longitudinal and transverse dispersivities values were 2 and 0.2 cm, respectively.

The solution composition of the water initially present in the soil profile is that of a highly sodic water: $Ca_T = 0.2$, $Na_T = 4.8$, $Cl_T = 4.6$, alkalinity = 0.4 mmol$_c$$L^{-1}$, with other concentrations equal to zero. The cation exchange capacity is 100 mmol$_c$$kg^{-1}$ ($\bar{C}a$ = 5.0, $\bar{N}a$= 95.0 mmol$_c$$kg^{-1}$). The Ca-Mg Gapon selectivity coefficient (K_{12} = 1.158) was taken from Wagenet and Hutson (1987). Two different irrigation water compositions were used. One water was almost gypsum-saturated: Ca_T = 32.6, $Na_T = 4.8$, $Cl_T = 5.0$, $SO_{4T} = 32.0$, alk = 0.4 mmol$_c$ L^{-1}, and zero for other concentrations. The second water is of the following composition: $Ca_T = 1.5$, $Na_T = 2.0$, $Cl_T = 1.0$, $SO_{4T} = 2.0$, alk = 0.5 mmol$_c$$L^{-1}$, and zero for other concentrations. Infiltration was attempted in three different ways. In the first case, gypsum-saturated water was applied to a soil without consideration of calcite dissolution. In the second case, high-quality water was applied to a soil, again, without consideration of calcite dissolution. In the third case, high-quality water was applied to a soil where the soil solution was in equilibrium with calcite. Cation exchange is treated as an instantaneous process.

Steady-state water flow was reached after approximately 1.5 days. Figure 5 shows the change in CO_2 concentration in space and time. The CO_2 concentration increases with time, with diffusion occurring predominantly in the direction of the dry furrow. The distribution of a hypothetical tracer is shown in Figure 6. The concentration front of the tracer reached a depth of approximately 1 meter after 1 day.

Figure 7 presents the exchangeable concentrations of calcium for the three scenarios after 5 days. There is a sharp exchange front (exchangeable sodium less than 10 %) reaching to approximately 70 cm for the gypsum water (Figure 7A). In contrast to Figure 7A, Figure 7B demonstrates penetration of the calcium front to a depth of less than 10 cm

when irrigating with the high-quality water. In this case, after 50 days the exchange front extended only to a depth of 40 cm (data not shown). Irrigation with the high-quality water, allowing for calcite equilibrium, showed a diffusive exchange front extending to a depth of 50 cm, with complete reclamation down to 15 cm (Figure 7C). Reclamation of the region below the furrow was essentially completed down to 1 meter after 25 days of leaching (data not shown).

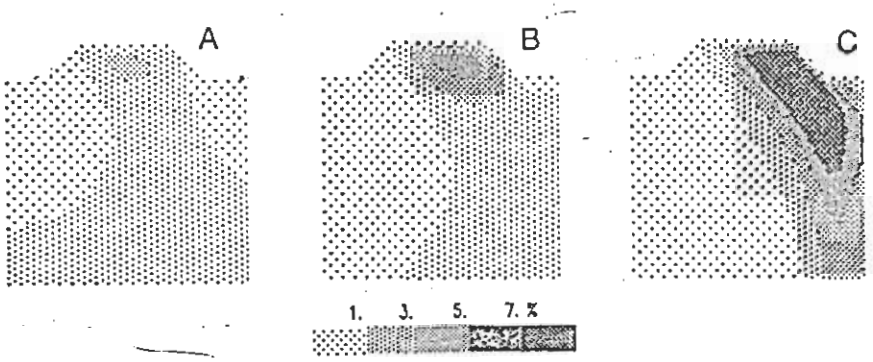

Figure 5. CO_2 concentration (%) profiles at different times for example 2: (A) 0.5, (B) 1, and (C) 5 days.

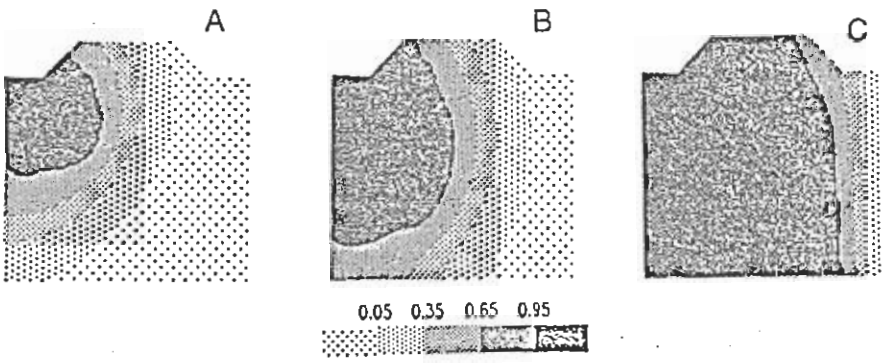

Figure 6. Tracer concentration profiles at different times for example 2: (A) 0.5, (B) 1, and (C) 5 days.

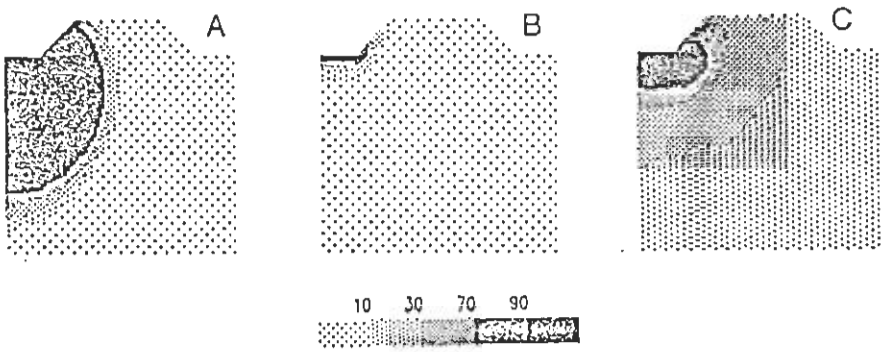

Figure 7. Exchangeable calcium concentration ($mmol_c kg^{-1}$) profiles after 5 days of infiltration: (A) infiltration with gypsum-saturated water, (B) infiltration with high-quality water, and (C) infiltration with high-quality water into profile containing calcite.

This figure demonstrates the importance of calcite dissolution during reclamation. Reclamation with calcite is often dismissed because of a lack of consideration of elevated CO_2 concentrations in the soil and the enhanced dissolution of calcite during the reclamation exchange. For example, calcite dissolution contributed 300 eq per m^2 of soil surface area to reclamation within the first 5 days of leaching. Selection of a higher exchange capacity and associated hydraulic properties of a finer-textured soil would increase both the time required for infiltration, and the quantity of water required for reclamation.

SUMMARY AND CONCLUSION

The SOILCO2 code, a process-based CO_2 production and transport model, combined with a variably saturated water flow model, was described. Comparison of the model to field data demonstrates its ability to predict both CO_2 concentrations in the soil and CO_2 fluxes to the atmosphere for a growing crop with changes in crop development, temperature, and soil water content. The multicomponent water and solute transport code UNSATCHEM-2D was also reviewed. This code is particularly suited for simulation of major ion solute chemistry of arid zone soils. The model considers the transport of CO_2, thus allowing for calculation of soil CO_2 concentrations. Soil CO_2 concentrations are used in the chemical subroutine to calculate solute composition. The model utilizes both extended Debye-Hückel and Pitzer activity coefficients; thus, it is suitable for use in extremely saline environments. The

chemistry subroutine includes both equilibrium and kinetic expressions for various solid phases. The reclamation example demonstrates the importance of elevated CO_2 concentrations combined with ion exchange in enhancing the solubility of calcite. Use of the model for reclamation and soil water management should enable more efficient use of amendments and water resources.

Future research will incorporate the chemistry and transport of oxyanions (such as boron, selenium, and arsenic) that are important when considering impacts of agricultural drainage waters in arid environments. In addition, a more detailed plant growth model will be incorporated to better predict plant response to environmental conditions.

REFERENCES

Bryant, SL, RS Schechter, and LW Lake. **1986.** Interactions of precipitation/dissolution waves and ion exchange in flow through permeable media. AIChE J 32:751-764.

Busenberg, E and LN Plummer. **1982.** The kinetics of dissolution of dolomite in CO_2-H_2O systems at 1.5 to 65 C and 0 to 1 ATM P_{co_2}. Am J Sci 282:45-78.

Buyanovsky, GA and GH Wagner. **1983.** Annual cycles of carbon dioxide level in soil air. Soil Sci Soc Am J 47:1139-1145.

Buyanovsky, GA, GH Wagner, and CJ Gentzer. **1986.** Soil respiration in a winter wheat ecosystem. Soil Sci Soc Am J 50:338-344.

Cederberg, GA, RL Street, and JO Leckie. **1985.** A groundwater mass transport and equilibrium chemistry model for multicomponent systems. Water Resour Res 21:1095-1104.

Celia, MA and ET Bououtas, and RL Zarba. **1990.** A general mass-conservative numerical solution for the unsaturated flow equation. Water Resour Res 26:1483-1496.

de Marsily, G. **1986.** *Quantitative Hydrology: Groundwater Hydrology for Engineers.* Academic Press, San Diego, CA.

Feddes, RA, PJ Kowalik, and H Zaradny. **1978.** *Simulation of Field Water Use and Crop Yield,* 188 pp. John Wiley, New York.

Felmy, AR and JH Weare. **1986.** The prediction of borate mineral equilibria in natural waters: Application to Searles Lake, California. Geochim Cosmochim Acta 50:2771-2783.

Förster, R and H Gerke. **1988.** Integration von Modellen des Wasser- und Stofftransports sowie physikochemischer Wechselwirkungen zur Analyse von Agrar-Ökosystemen. Verhandlungen der Gesellschaft für Ökologie, Band XVIII, Essen.

Gilmore, E and JS Rogers. **1958.** Heat units as a method of measuring maturity in corn. Agron J 50:611-615.

Glinski, J and W Stepniewski. **1985.** *Soil Aeration and Its Role for Plants*. CRC Press, Boca Raton, FL.

Gureghian, AB. **1981.** A two-dimensional finite-element solution for the simultaneous transport of water and multisolutes through a nonhomogeneous aquifer under transient saturated-unsaturated flow conditions. Sci Tot Environ 21:329-337.

Huyakorn, PS, JB Kool, and YS Wu. **1991.** *VAM2D - Variably Saturated Analysis Model in Two Dimensions, Version 5.2 with Hysteresis and Chained Decay Transport, Documentation and User's Guide*, NUREG/CR-5352, Rev 1. US Nuclear Regulatory Commission, Washington, DC.

Inskeep, WP and PR Bloom. **1985.** An evaluation of rate equations for calcite precipitation kinetics at pCO_2 less than 0.01 atm and pH greater than 8. Geochim Cosmochim Acta 49:2165-2180.

Inskeep, WP and PR Bloom. **1986.** Kinetics of calcite precipitation in the presence of water-soluble organic ligands. Soil Sci Soc Am J 50:1167-1172.

Jennings, AA, DJ Kirkner, and TL Theis. 1982. Multicomponent equilibrium chemistry in groundwater quality models. Water Resour Res 18:1089-1096.

Kirkner, DJ, AA Jennings, and TL Theis. 1985. Multisolute mass transport with chemical interaction kinetics. J Hydrol 76: 107-117.

Liu, CW and TN Narasimhan. **1989.** Redox-controlled multiple-species reactive chemical transport. 1. Model development. Water Resour Res 25:869-882.

Logan, SH and PB Boyland. 1983. Calculating heat units via a sine function, J Am Soc Hortic Sci 108:977-980.

Mangold, DC and C-F Tsang. 1991. A summary of subsurface hydrological and hydrochemical models. Rev Geophys 29:51-79.

Ouyang, Y and L Boersma. 1992. Dynamic oxygen and carbon dioxide exchange between soil and atmosphere: I. Model development. Soil Sci Soc Am J 56:1695-1702.

Patwardhan, AS, JL Nieber, and ID Moore. 1988. Oxygen, carbon dioxide, and water transfer in soils: mechanism and crop response. Trans ASEA 31:1383-1395.

Pitzer, KS. 1979. Theory: Ion interaction approach. Chapter 7. In: *Activity Coefficients in Electrolyte Solutions*, Volume I, RM Pytkowicz, ed. CRC Press, Boca Raton, FL.

Plummer, LN, TM Wigley, and DL Parkhurst. 1978. The kinetics of calcite dissolution in CO_2 systems at 5 to 60C and 0.0 to 1.0 atm CO_2. Am J Sci 278:179-216.

Rawls, WJ, DL Brakensiek, and KE Saxton. 1982. Estimation of soil water properties. Trans ASAE 25:1316-1320.

Rixon, AJ. 1968. Oxygen uptake and nitrification at various moisture levels by soils and mats from irrigated pastures. J Soil Sci 19:56-66.

Robbins, CW, RJ Wagenet, and JJ Jurinak. 1980a. A combined salt transport-chemical equilibrium model for calcareous and gypsiferous soils. Soil Sci Soc Am J 44:1191-1194.

Robbins, CW, RJ Wagenet, and JJ Jurinak. 1980b. Calculating cation exchange in a salt transport model. Soil Sci Soc Am J 44:1195-1200.

Šimůnek, J, T Vogel, and M Th van Genuchten. 1992. *The SWMS_2D Code for Simulating Water Flow and Solute Transport in Two-Dimensional Variably Saturated Media, Version 1.1*, Research Report No. 126. US Salinity Laboratory, USDA, ARS, Riverside, CA.

Šimůnek, J and DL Suarez. 1993a. Modeling of carbon dioxide transport and production in soil: 1. Model development. Water Resour Res 29:487-497.

Šimůnek, J and DL Suarez. 1993b. *The UNSATCHEM-2D Code for Simulating Two-Dimensional Variably Saturated Water Flow, Heat*

Transport, Carbon Dioxide Transport, and Solute Transport with Major Ion Equilibrium and Kinetic Chemistry, Version 1.1, Research Report No. 128. US Salinity Laboratory, USDA, ARS, Riverside, CA.

Šimůnek, J and M Th van Genuchten. **1994.** The CHAIN_2D code for simulating two-dimensional movement of water, heat and multiple solutes in variably-saturated soils, Research Report No. 136. US Salinity Laboratory, USDA, ARS, Riverside, CA.

Šimůnek, J and DL Suarez. **1994.** Two-dimensional transport model for variably saturated porous media with major ion chemistry. Water Resour Res 30:1115-1133.

Stumm, W and JJ Morgan. **1981.** *Aquatic Chemistry: An Introduction Emphasizing Chemical Equilibria in Natural Waters*. John Wiley, New York.

Suarez, DL. **1977.** Ion activity products of calcium carbonate in waters below the root zone. Soil Sci Soc Am J 41:310-315.

Suarez, DL. **1985.** Prediction of major ion concentrations in arid land soils using equilibrium and kinetic theories, pp. 107-175. In: ARS Modeling Symposium, USDA-ARS-30, D. G. DeCoursey, ed. US Department of Agriculture, Pingree Park, CO.

Suarez, DL. **1994.** Carbonate chemistry of computer programs and their application to soil chemistry. In: *Chemical Equilibrium and Reaction Models*, RH Loeppert, ed. Soil Sci Soc Am Special Publication, Madison, WI.

Suarez, DL and JD Rhoades. **1982.** The apparent solubility of calcium carbonate in soils. Soil Sci Soc Am J 46:716-722.

Suarez, DL and J Šimůnek. **1993.** Modeling of carbon dioxide transport and production in soil: 2. Parameter selection, sensitivity analysis and comparison of model predictions to field data. Water Resour Res 29:499-513.

Suarez, DL and J Šimůnek. (in preparation). Modeling major ion equilibrium and kinetic chemistry coupled to unsaturated water flow and solute transport, Soil Sci Soc Am J.

Truesdell, AH and BF Jones. **1974.** Wateq, a computer program for calculating chemical equilibria of natural waters. J Res US Geol Surv 2:233-248.

Valocchi, AJ, RL Street, and PV Roberts. **1981.** Transport of ion-exchanging solutes in groundwater: Chromatographic theory and field simulation. Water Resour Res 17:1517-1527.

van Genuchten, M Th. **1987.** *A Numerical Model for Water and Solute Movement in and Below the Root Zone*, Unpublished research report. US Salinity Laboratory, USDA, ARS, Riverside, CA.

Wagenet, RJ and JL Hutson. **1987.** LEACHM: *L*eaching *E*stimation *A*nd *CH*emistry *M*odel, A Process-Based Model of Water and Solute Movement, Transformations, Plant Uptake and Chemical Reactions in the Unsaturated Zone, *Continuum 2*. Water Resource Institute, Cornell University, Ithaca, NY.

Walsh, MP, SL Bryant, RS Schechter, and LW Lake. **1984.** Precipitation and dissolution of solids attending flow through porous media. AIChE J 30:317-328.

White, N and LW Zelazny. **1986.** Charge properties in soil colloids, Chapter 2, pp. 39-77. In: *Soil Physical Chemistry*, DL Sparks, ed. CRC Press, Boca Raton, FL.

Williams, ST, M Shameemullah, ET Watson, and CI Mayfield. **1972.** Studies on the ecology of actinomycetes in soil. IV, The influence of moisture tension on growth and survival. Soil Biol Biochem 4:215-225.

Yeh, GT and DD Huff. **1985.** *FEMA: A Finite Element Model of Material Transport Through Aquifers*, ORNL-6063. Oak Ridge National Laboratory, Oak Ridge, TN.

Yeh, GT and VS Tripathi. **1989.** A critical evaluation of recent developments in hydrogeochemical transport models of reactive multichemical components. Water Resour Res 25:93-108.

Yeh, GT and VS Tripathi. **1991.** A model for simulating transport of reactive multispecies components: Model development and demonstration. Water Resour Res 27:3075-3094.